JMEPEG (2023) 32:4922–4931
https://doi.org/10.1007/s11665-022-07446-4

1059-9495/$19.00

TECHNICAL ARTICLE

Ultrafine Carbide-Free Bainite in High-Carbon Steel After Continuous Annealing with Different Cooling Rates

Behzad Avishan, Roya Karimkhani Shamloo, Elina Akbarzadeh Chiniforoush, and Sasan Yazdani

Submitted: 14 June 2022 / Revised: 30 August 2022 / Accepted: 9 September 2022 / Published online: 30 September 2022

In addition to conventional isothermal heat treatment, ultrafine carbide-free bainite can be obtained by continuous annealing of steels, which is of great interest to scientists and research communities. The resulting microstructure consists of bainitic sheaves composed of bainitic ferrites interwoven with austenite films in nanoscale, being separated by austenite microblocks resulting in GPa-strength level. This article aims to investigate the microstructural characteristics and impact toughness of high-carbon steel after continuous cooling heat treatment at cooling rates of 0.1, 0.15, 0.2 and 0.3 °C/min. Results indicated that bainitic ferrites and austenite films of less than 270 nm and different volume fractions of bainitic sheaves and high carbon retained austenite could be attained. Wider size distribution of bainitic ferrites was achieved by a slower cooling rate due to the progressive transformation of the primary austenite to bainite. Finally, it has been shown that impact toughness values were increased by decreasing the cooling rate of the steel due to a more effective TRIP effect and obtaining more bainitic sheaves with different orientations, while premature bainite transformation and the presence of martensite deteriorated the impact toughness when the highest cooling rate was applied.

Keywords carbide-free bainite, continuous annealing, fracture toughness, heat treatment, microstructure, steel

1. Introduction

The heat treatment process and the determination of the proper heat treatment parameters like temperature, time and cooling rate are important variables that must be taken in to account for developing steels with desirable microstructural characteristics and mechanical properties. Microstructural features such as ferrite, pearlite, bainite and martensite can be obtained based on the hardenability of the steel and the heat treatment cycle being applied. While a ferritic microstructure provides improved ductility, martensite formation within the microstructure results in a very strong and brittle engineering product. Considering that a composite microstructure containing various volume fractions of different phases can also be achieved by an appropriate heat treatment, it is crucial to control the heat treatment cycle and consequently the volume fractions and morphologies of the phases to achieve the expected mechanical properties.

Bainite morphology is an ideal microstructure that exhibits valuable mechanical properties in many engineering applications where high wear resistance, strength, and fatigue properties are important (Ref 1). Due to the wide temperature range in which bainitic transformation occurs, various bainite morphologies can be obtained. Accordingly, classical upper and lower bainite can be achieved, with bainitic ferrites and cementite precipitates being the main microstructural constituents with different contributions (Ref 1, 2) However, cementite has a significant effect on reducing toughness and ductility properties in bainitic steels, especially when it is coarse in morphology and has a high volume fraction. This is the reason for the higher toughness in lower bainite compared to upper bainite due to the finer cementite precipitates in the microstructure. In this regard, replacement of the brittle cementite phase with a more ductile microstructural constituent would be beneficial in enhancement of the ductility. The demands for producing bainitic steels with improved strength and ductility properties resulted in the introduction of a new class of bainite, called carbide-free bainite (CFB), in which carbide precipitation was restricted and replaced with ductile high carbon retained austenite within the microstructure (Ref 3, 4). Transformation induced plasticity (TRIP) effect occurs during straining the sample and leads to modified strength—ductility combination (Ref 5, 6). On the other hand, a new generation of CFB, known as Nanostructured Low-Temperature Bainitic Steels (NLBS) has gained considerable attention during the last two decades due to their GPa-strength level and significant ductility balance depending on the heat treatment process (Ref 7-12). These steels meet the engineering requirements such as high strength levels, low yield to tensile strength ratio and significant combination of strength and elongation for high technology demands (Ref 13). NLBS belongs to the third generation of advanced high strength steels (AHSS) and its advanced mechanical properties are the result of a simple isothermal heat treatment that is being applied to steel with sufficient hardenability and there is no need for complicated manufacturing processes (Ref 14). The temperature and time of bainite transformation are two critical variables that

Behzad Avishan, Department of Materials Engineering, Azarbaijan Shahid Madani University, Tabriz, Iran; and **Roya Karimkhani Shamloo, Elina Akbarzadeh Chiniforoush,** and **Sasan Yazdani**, Faculty of Materials Engineering, Sahand University of Technology, Tabriz, Iran. Contact e-mails: avishan@azaruniv.ac.ir and yazdani@sut.ac.ir.

must be carefully considered in the production of NLBS, as they have a significant effect on the microstructural features, size, and volume fraction, and thus on the resulting mechanical properties (Ref 15). Bainitic subunits less than 300 nm thick are the main contributing factor for the high strength level in these steels, and the volume fraction and morphology of the high carbon retained austenite principally control the ductility (Ref 11, 16, 17). However, the role of austenite in strength properties cannot be ignored. While retained austenite decreases the yield strength, the transformation of austenite to martensite during straining the sample increases the tensile strength through the TRIP effect (Ref 13, 18, 19). It has been approved that a modified mechanical stability of austenite is mandatory to achieve the desired mechanical properties and austenite morphology is an important parameter that must be controlled (Ref 12, 20, 21). In this case, it would be beneficial to replace austenite blocks with austenite films and reduce the existing block sizes as much as possible. This is the point where the heat treatment cycle and the production process play an important role and need to be carefully designed.

Conducting a multi-step isothermal austempering heat treatment has been suggested as an effective approach to reduce the number of austenite blocks and increase the volume fraction of bainitic sheaves where it has been reported also to result in modification of the mechanical properties (Ref 22-26) However, it is not always possible to apply an isothermal heat treatment process to an engineering material, and the production rout may involve continuous cooling, where the steel passes through a temperature range between the bainite start (Bs) and martensite start (Ms) temperatures continuously. This is the point at which the cooling rate is important, and the microstructural characteristics vary depending on the heat treatment cycle. Accordingly, it is important to have information about the continuous cooling transformation (CCT) diagram of steel to predict the possible variations in microstructural features. The CCT diagram of the steel depends mainly on the chemical composition. Carbon is the main alloying element in NLBS with almost 0.8-1 wt.%, which successfully increases the hardenability. Mn and Cr are also being added to these steels, which are useful to achieve nano scale bainite even at low cooling rates. Furthermore, the addition of Mn and Cr adjusts the T_o-curve to higher carbon concentrations, which in turn higher volume fraction of bainite can be achieved at any transformation temperature (Ref 27).

There are several reports evaluating the microstructural characteristics and mechanical response of CFB steels during the continuous cooling process, where the materials were generally low and medium carbon steels. Caballero et al. (Ref 13) designed CFB steel by cold rolling and subsequent continuous annealing heat treatment and reported that an optimum balance between strength and ductility could be achieved, making the material potential to be used in many engineering applications. It has been confirmed that higher uniform elongation could be achieved compared to that of dual-phase and martensitic steels with similar strength levels. Gomez et al. (Ref 28) studied the microstructural features and mechanical properties of CFB obtained after continuous cooling transformation in steels with carbon contents between 0.24 and 0.35 wt.%, and results indicated that very fine microstructural features and promising mechanical properties could be obtained if the formation of the blocky austenite morphology was avoided. Chen et al. (Ref 29) showed that dynamic continuous cooling of medium carbon steel resulted in CFB with sufficiently high strength and toughness properties when the volume fraction of retained austenite decreased with decreasing cooling rate. Morales-Rivas and co-workers (Ref 30) studied the microstructural bandings in continuously cooled CFB and it has been indicated that despite the formation of microstructural banding, the bainite morphology did not change from the bands to the matrix and a higher proportion of martensite and deformed austenite was found in the bands. It has been explained that the band formation had little effect on the mechanical properties. Caballero et al. (Ref 31, 32) confirmed the possibility of obtaining unprecedented strength and ductility properties in medium carbon CFB steels after continuous cooling transformation. It has been declared that the strength and ductility of the CFB steels were comparable to those of maraging steels, while the production costs were thirty times lower. In another study (Ref 33), CFB could be obtained after coiling and air cooling procedures in steels with carbon content between 0.27 and 0.3 wt.% and the effect of the morphology of the retained austenite and its stability on the ductility of the materials have been investigated. It has been shown that the CFB obtained after coiling contained coarse and blocky bainite morphology, which resulted in a higher uniform deformation value comparing to the samples heat-treated by air cooling with very fine bainite platelets in the microstructure. Finally, Clyton and Jin (Ref 34) confirmed that CFB steels could be produced in low and medium carbon steels by continuous cooling transformation, showing improved wear behavior comparable to that of Hadfield′s manganese steel.

When steel is subjected to continuous cooling below Bs and above Ms temperatures, the volume fractions of the bainitic sheaves and high carbon retained austenite, as well as the size distributions of bainitic subunits, austenite films and austenite microblocks may diverge. Bainitic transformation occurs continuously, and austenite progressively transforms into bainite, leading to an increase in the volume fraction of bainite and preventing the retention of large retained austenite regions within the microstructure. However, the bainitic ferrites and austenite films within the bainitic sheaves that form at each temperature may vary in thickness. This would affect the resulting mechanical response of the material. Although different information is available on the continuous cooling of low and medium carbon steels to obtain bainite in the microstructure, there is lack of data on the continuous cooling of high carbon steels and the resulting microstructural characteristics and mechanical properties. In this work, the microstructural characteristics and impact toughness of high carbon steel with sufficient hardenability has been investigated after continuous cooling at different cooling rates between 0.1 and 0.3 °C/min.

2. Material and Methods

An induction furnace was used to cast 10 kg of primary steel in a rectangular shape and the chemical composition of the steel was designed based on the thermodynamic theories of bainite transformation (Ref 1). The cast steel was electro slag remelted in order to eliminate the inclusions as much as possible and hot-rolled after homogenizing at 1200 °C for 5 h to achieve a wrought steel. The final chemical composition of the steel is given in Table 1. It contains sufficient C for hardenability, Si and Al to suppress carbide precipitation (Ref 35, 36), Mn and

Cr to improve hardenability, Mo to prevent temper embrittlement due to phosphorus (Ref 37), and Co and Al to increase the transformation rate of bainite (Ref 38).

The hot-rolled sheet was machined on both sides to remove the decarburized layers and to obtain parallel surfaces with a final thickness of 15 mm. Test samples were cut from the sheet using an electric discharge machine and austenitized in a salt bath furnace at 900 °C for 30 min, immediately quenched in another salt bath furnace at 400 °C and held for 3 min to avoid diffusional phase transformation products formation and to achieve a uniform temperature at each point of the test material. They were then continuously cooled to ambient temperature (25 °C) in a tube furnace at cooling rates of 0.1, 0.15, 0.2 and 0.3 °C/min. The schematic representation of the different processing stages after casting and electro slag remelting can be seen in Fig. 1. The annealing rates were selected based on data predicted by the JMatPro™ software, which roughly estimated the CCT diagram of the steel and its theoretical Ms temperature.

Kinetics samples of 10 × 5 × 5 mm^3 were used to evaluate the progress of bainite transformation. Microstructural characterization was carried out using the Olympus PMG3™ optical and Tescan MIRA3™ field emission scanning electron (FE-SEM) microscopes. Samples were grinded and polished according to standard procedures and etched with a 2% Nital etching solution. Image analysis was performed at different positions in kinetics samples and the high magnification FE-SEM images were used to determine the thickness and size of the bainitic ferrite and austenite films using the line-intercept method (Ref 39). Moreover, the size distributions of bainitic ferrites were examined using at least ten FE-SEM images after 8-10 measurements in each image.

Table 1 The final chemical composition (wt.%) of the steel after casting, ESR, homogenizing and hot rolling procedures

C	Si	Mn	Cr	Mo	Co	Al	Fe
0.92	1.58	2.25	1.33	0.27	1.4	3.04	Balance

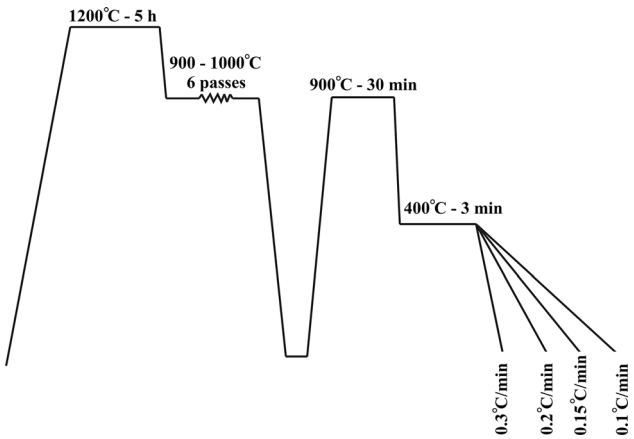

Fig. 1 Schematic illustration of the different processing stages after casting and electro slag remelting

X-ray diffraction was used to determine the volume fraction of the high carbon retained austenite within the microstructure. Scanning was performed on a Bruker-D8 Advance™ diffractometer using CuKα radiation at 40 kV and 40 mA and a scan range of 40-105°. Step size and counting time were 0.3° and 4 s/step, respectively. The volume fraction of retained austenite was calculated using the integrated intensities of the (200), (220) and (311) peaks of austenite and the (200), (211) and (220) peaks of ferrite (Ref 40). XRD profile refinements were also performed to measure the carbon content of the austenite according to the method described by Dyson and Holmes (Ref 41).

Vickers hardness measurements were performed according to the ASTM-EM92 standard method with a load of 30 kg and the mean values of at least 4 measurements were reported for each heat treatment condition. Finally, the Charpy impact toughness of the heat-treated specimens was determined using V-notched samples of 10 × 10 × 55 mm^3 in size. At least three specimens were used for each heat treatment condition to ensure the reproducibility. The fracture surfaces of the test specimens were examined with scanning electron microscope.

3. Results and Discussions

Figure 2 illustrates the CCT diagram of the primary steel including the pearlite and bainite regions and it can be seen that the steel had sufficient hardenability to prevent the formation of diffusional phase transformation products, i.e. pearlite morphologies, during quenching of the samples from the austenitizing temperature into the salt bath furnace at 400 °C. Based on the data obtained from the CCT diagram, it would take more than 100 min at 400 °C for the bainite transformation to start and this would allow the austenite phase to remain stable before starting the continuous cooling processes with different cooling rates. This was confirmed experimentally by quenching a sample in water after austenitizing and quenching to 400 °C and holding for 3 min before starting the continuous process of heat treatments. The microstructure of the steel was martensitic with a hardness value of 644 ± 10 HV30. Theoretical simulations predicted that cooling rates of more than 1 °C/min were

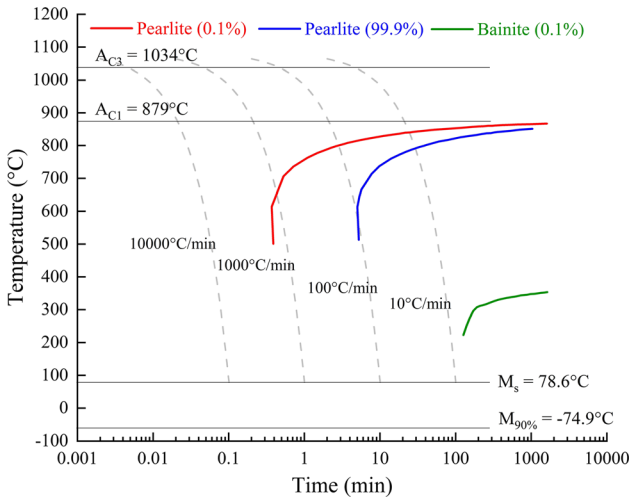

Fig. 2 The CCT diagram of the steel roughly estimated using the JMatPro™ software

required for bainite transformation in the test samples and it would not be possible to produce bainite at lower cooling rates after immediate quenching to 400 °C with a holding time of 3 min.

The microstructural features of continuously cooled specimens with various cooling rates of 0.3, 0.2, 0.15 and 0.1 °C/min are shown in Fig. 3. Initial evaluations showed that bainitic sheaves (dark features) and austenite/martensite (γ/M) microblocks (light features) were the main microstructural constituents with different volume fractions depending on the cooling rates. The volume fraction of the bainitic sheaves and γ/M microblocks were roughly estimated by IMAGE J software and results indicated that almost 57, 68, 78 and 89% of bainitic sheaves and 43, 32, 25 and 16% of γ/M microblocks were present within the microstructure of the samples at the end of the cooling rates of 0.3, 0.2, 0.15 and 0.1 °C/min, respectively. Again, the microstructural characterization confirmed that there was no evidence of any diffusional phase transformation products that might form during the transfer of the samples from the austenitizing furnace to the 400 °C salt bath furnace. This indicates a sufficiently high hardenability of the steel and a high cooling rate during the transfer of the samples from the austenitizing furnace to the 400 °C furnace before the continuous bainitic transformation begins. While the lowest amount of bainite formed at a cooling rate of 0.3 °C/min, a decrease in the cooling rate led to the formation of more bainitic sheaves within the microstructures. The γ/M microblocks separated the bainitic sheaves and their volume fractions and sizes decreased with decreasing cooling rate. Considering that the samples were cooled continuously from 400 °C to an ambient temperature of 25 °C, it would take about 20, 30, 40 and 60 h for the cooling process to complete and bainite transformation to occur at cooling rates of 0.3, 0.2, 0.15 and 0.1 °C/min, respectively. The samples cooled at the lowest cooling rate had sufficient time for bainite transformation, and a higher proportion of the primary austenite phase gradually transformed into bainite. As a result, a higher volume fraction of bainite was obtained, which was separated with fewer and smaller austenite microblocks, as shown in Fig. 3(d). In contrast, at higher cooling rates, the steel rapidly passes through the temperature range between Bs and Ms and the bainite transformation does not have sufficient time to complete. It would therefore be logical to achieve a lower bainite content in the microstructure, which is more pronounced at the highest cooling rate of 0.3 °C/min.

In general, the volume fraction of bainite formed in the microstructure directly affects the amount of the high carbon retained austenite that is stable in the CFB at room temperature. The transformation of austenite to bainite starts by paraequilibrium nucleation of bainitic ferrites from primary austenite grain boundaries and it progresses by shear growth of the bainitic subunits (Ref 1, 42-46). Carbon partitions to the surrounding austenite according to its low solubility in ferrite and remains in solid solution in austenite because Si and Al forbid carbon precipitation as cementite. Almost 0.5-1 wt.%

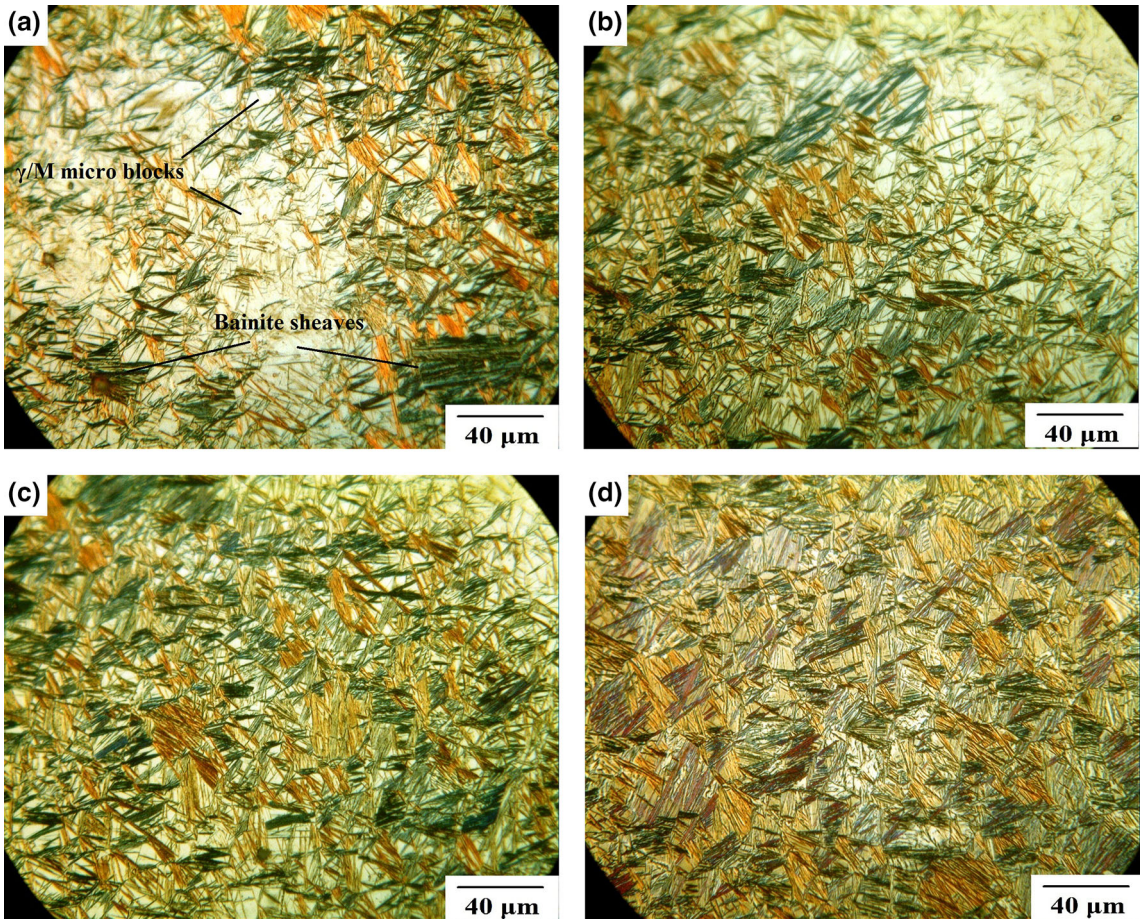

Fig. 3 Optical images of the samples cooled continuously at (a) 0.3 °C/min, (b) 0.2 °C/min, (c) 0.15 °C/min, and (d) 0.1 °C/min showing the bainitic sheaves (dark features) and γ/M microblocks (light features)

carbon is required in solid solution for austenite to be thermally stable at room temperature (Ref 47). When a smaller amount of bainite forms, the carbon rejection is not considerable to stabilize the austenite phase, and a larger amount of austenite transforms to martensite during cooling to the room temperature. However, at lower cooling rates, where greater amount of bainitic sheaves form from the primary austenite, the remaining austenite phase is sufficiently enriched in carbon due to the more severe carbon partitioning and this results in retention of a higher volume fraction of austenite surrounding the bainitic sheaves. So, it was logical to assume that the different cooling rates would affect the amount of austenite within the final microstructure of the samples, as can be seen in the XRD profiles in Fig. 4. Ferrite and austenite peaks were identified with different intensities and results of the profile refinements have been summarized in Table 2. The experimental results indicated that almost 45, 47, 58, 50% volume fraction of thermally stable high carbon retained austenite could be gained at the end of the 0.1, 0.15, 0.2 and 0.3 °C/min cooling rates, respectively. It was difficult to distinguish the bainitic ferrite and martensite peaks in the XRD profiles, because of the overlapping of the peaks appearing at same 2θ°.

At a continuous cooling rate of 0.3 °C/min, the lowest volume fraction of bainite formation resulted in the austenite phase having the lowest carbon content, which was calculated to be nearly 0.55 wt.% (see Table 2). Accordingly, the Ms temperature of the austenite was roughly estimated to be close to 281 °C (according to the MUCG83™ software (Ref 48)), implying that transformation of austenite to martensite was inevitable during continuous cooling to the room temperature. The final microstructure contained bainitic sheaves, high carbon retained austenite and martensite. However, when the cooling rate decreased to 0.2 °C/min, the austenite became more carbon enriched due to the higher volume fraction of bainite formation, and 0.7 wt.% carbon in solid solution in the austenite decreased the Ms temperature to 199 °C. Therefore, the martensite phase was partially replaced with bainite and high carbon retained austenite and the remaining austenite was more stable to resist transforming to martensite during cooling to the room temperature compared to that of 0.3 °C/min cooling rate. For this reason, the volume fraction of austenite increased to almost 58%. Implementing the 0.15 and 0.1 °C/min cooling rates made it possible for further progressive transformation of austenite phase to bainite and consequently the volume fraction of austenite reduced being more evident

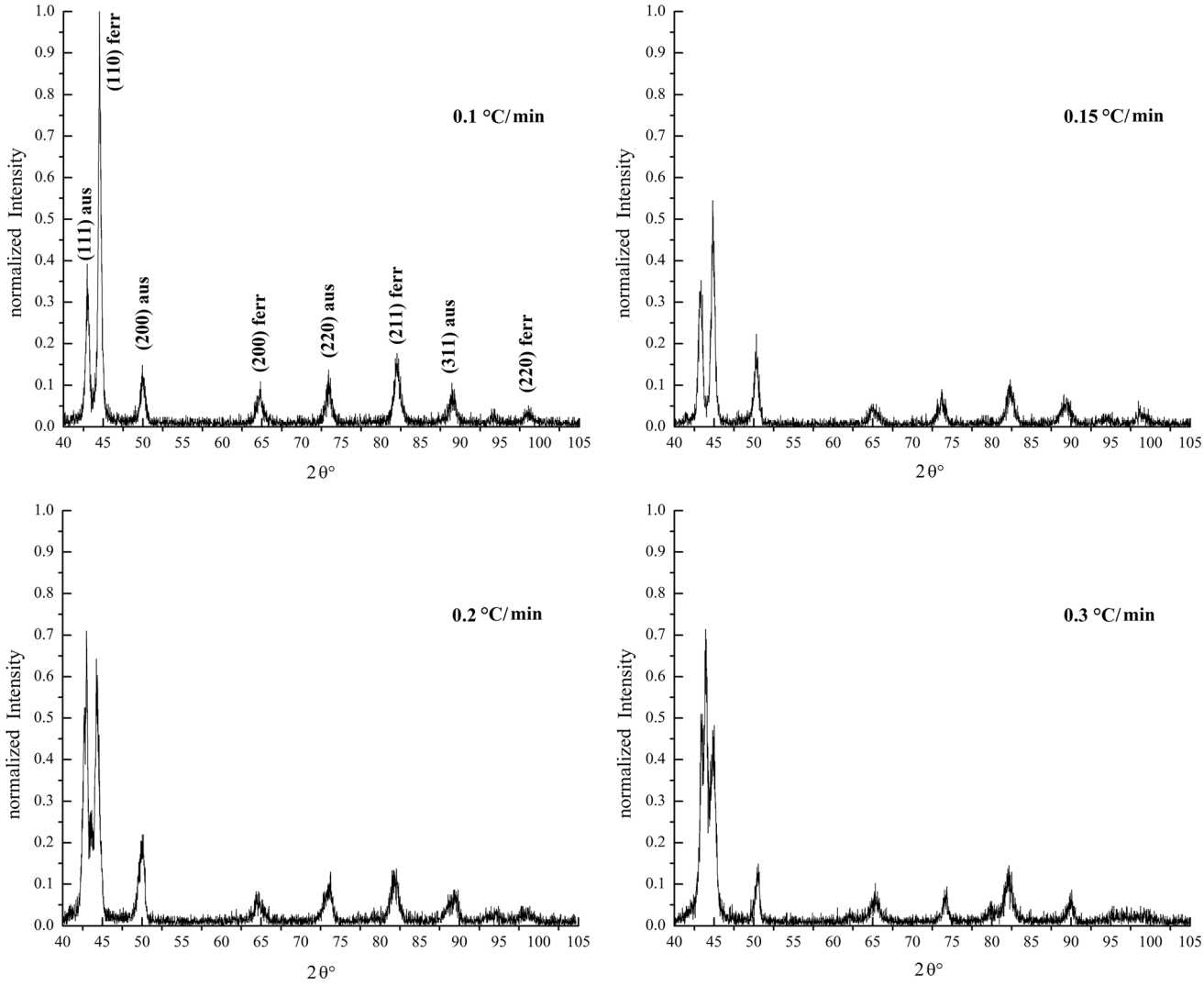

Fig. 4 XRD profiles for samples continuously cooled at different cooling rates

Table 2 Volume fraction of austenite and hardness values for samples heat treated at different conditions

	Cooling rate			
	0.3 °C/min	**0.2 °C/min**	**0.15 °C/min**	**0.1 °C/min**
Austenite content (%)	50.13	58.38	47.57	45.65
Austenite carbon content (wt.%)	0.55	0.70	0.87	1.37
Martensite start temperature (°C)	281	199	145	− 104

when the transformation rate was 0.1 °C/min. The highest amount of bainitic sheaves formed at the end of the 0.1 °C/min cooling rate and the retained austenite enriched which the highest amount of carbon in the solid solution (1.37 wt.%), which made the austenite enough stable not to transform into martensite during cooling to the ambient temperature. The Ms temperature was estimated to be close to −104 and it was impossible to achieve martensite after cooling the samples to the ambient temperature. The final microstructure contained the highest volume fraction of bainite separated by austenite microblocks. It should be mentioned that the XRD method is not as accurate as other methods such as APT (atomic probe tomography) in determining the carbon content of the retained austenite and consequently calculating the Ms temperature. However, it can provide values that are close to reality with small errors.

Optical images were not able to distinguish the bainitic ferrites interwoven with austenite films within each bainitic sheave. Therefore, FE-SEM images with high magnifications were used to determine the thickness of these phases and to evaluate the transformation progress examples of which have been given in Fig. 5. According to the results, each sheaf contained parallel layers of bainitic ferrites and austenite films, and γ/M microblocks were distributed in the microstructure separating the bainitic sheaves. The volume fraction and mean diameter of the γ/M microblocks were lower for samples heat-treated at lower cooling rates due to the consumption of more primary austenite and the formation of a higher volume fraction of bainite. Considering the scale of the microstructure, results showed that bainitic subunits with a thickness of less than 220 nm and austenite films with a thickness of less than 265 nm could be obtained depending on the cooling rate, as summarized in Table 3. Bainitic ferrites of nearly 92, 124, 175 and 218 nm and austenite films of nearly 165, 212, 233 and 265 nm could be obtained at the end of the continuous cooling rates of 0.3, 0.2, 0.15 and 0.1 °C/min, respectively. The results can be justified considering that the temperature at which bainite forms strongly affects the thickness of the subunits and enough time is required for bainite transformation at each transformation temperature (Ref 49). Primary austenite is much stronger at lower transformation temperatures and restricts the motion of the glissile interface of the ferrite/austenite, resulting in thinner bainitic subunits. In contrast, increasing the heat treatment temperature would result in thicker phase constituents. At a lower continuous cooling rate, the sample passes through a wide range of transformation temperatures more gradually and there is enough time for bainite transformation. Therefore, bainitic ferrites of different sizes can be formed at each transformation temperature step, allowing for a wider size distribution of bainitic ferrites and bigger mean thickness value. Bainitic ferrites formed at higher transformation temperatures further enrich the austenite with more carbon, which lowers the Bs and Ms temperatures of the remaining austenite and increases the driving force of the bainite transformation and consequently, higher amount of bainite can be achieved. However, increasing the cooling rate makes bainite transformation more difficult at each subsequent temperature step, resulting in a narrower size distribution because of a pre-mature bainite transformation. Figure 6 shows the size distribution of the bainitic ferrites within the microstructures of the samples at the end of the different continuous cooling rates. Results showed that the standard deviations for the mean values of the bainitic ferrite thicknesses were larger at lower cooling rates due to the wider size distributions and the formation of bainite at different temperatures with different thicknesses.

The volume fraction and thickness of the bainitic ferrite plates are the main factors controlling the hardness value of the steel with a completely bainitic microstructure. Higher hardness values would be attained when higher volume fractions and finer bainitic subunits are present in the microstructure (Ref 8). However, the possibility of the presence of martensite and its volume fraction must also be considered when describing the hardness values of the specimens in this study. The hardness values are summarized in Table 3 and it is obvious that the highest hardness value was obtained at the highest cooling rate of 0.3 °C/min, at which the least amount of bainite formed with the lowest thickness value and the highest volume fraction of martensite was present in the microstructure. Reducing the cooling rate from 0.3 to 0.2 and 0.15 °C/min made it possible for harder martensite to be replaced with bainitic ferrite and austenite phases, which in turn led to a decrease in hardness from 570 to 507 and 480 HV30, respectively, apart from the fact that the bainitic subunits were thicker. Considering the competitive role of martensite and bainite sheaves in affecting the hardness in the specimens, the lowest hardness value could be achieved when the steel was cooled continuously at a cooling rate of 0.1 °C/min with the highest volume fraction of bainite with the thickest bainitic subunits and the insignificant fraction of martensite.

The volume fraction of the high carbon retained austenite phase and its morphology must be considered as the main parameters determining ductility in CFB. Meanwhile, it is critical to consider the volume fraction of martensite and bainitic sheaves to evaluate the impact toughness values of the specimens (Ref 50). Table 3 shows that the impact toughness of the heat-treated samples increased from 8 to 11, 15 and 19 J when the cooling rate decreased. A continuous cooling rate of 0.3 °C/min resulted in a high proportion of martensite and the lowest volume fraction of bainite in the microstructure of the sample, and the negative role of brittle martensite dominated the effectiveness of the high carbon austenite phase in promoting ductility. Moreover, the austenite phase present

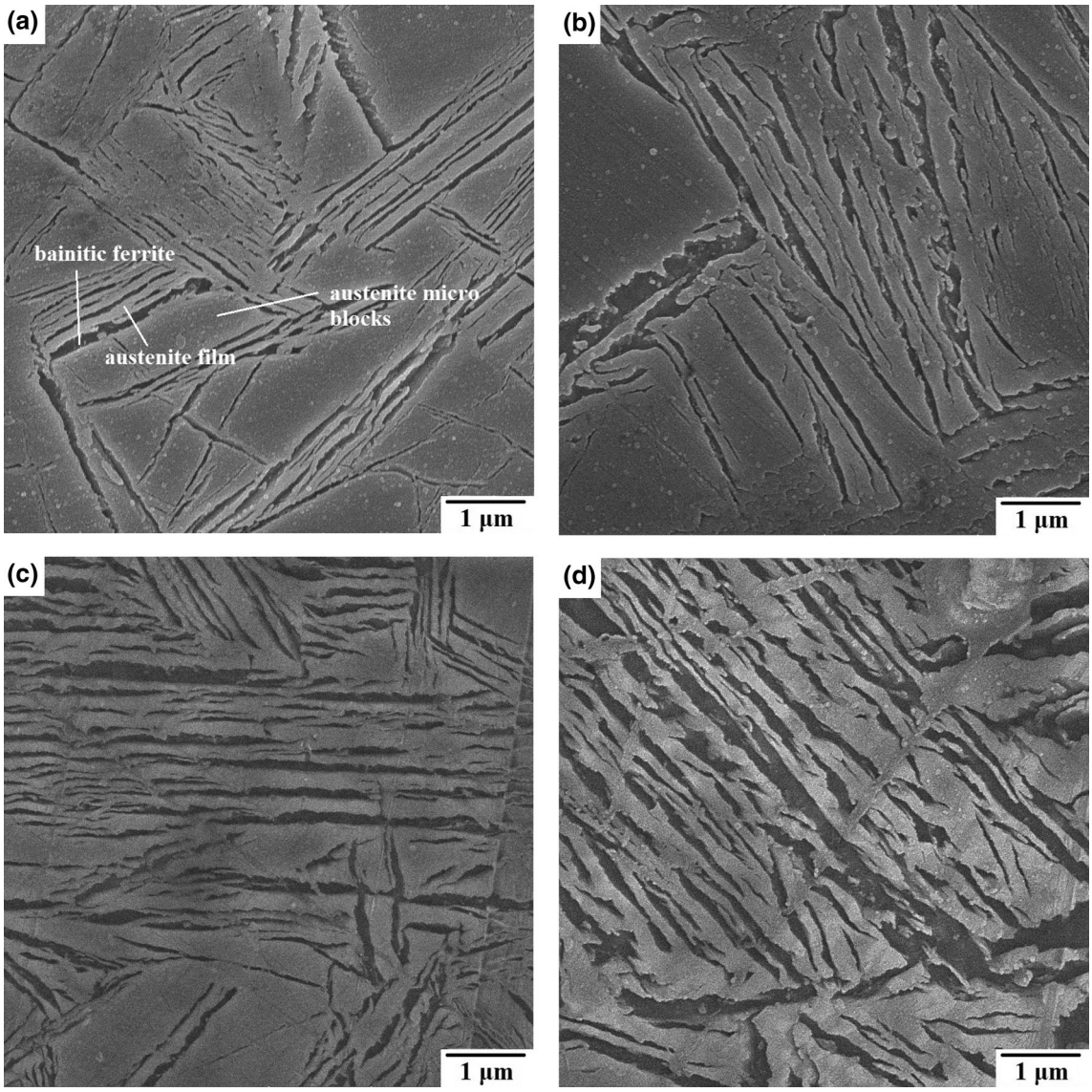

Fig. 5 FE-SEM images of the samples continuously cooled at (a) 0.3 °C/min, (b) 0.2 °C/min, (c) 0.15 °C/min and (d) 0.1 °C/min

Table 3 The thickness of the bainitic ferrites and austenite films in samples heat-treated at different conditions

	Cooling rate			
	0.3 °C/min	**0.2 °C/min**	**0.15 °C/min**	**0.1 °C/min**
Thickness of bainitic ferrites (nm)	92 ± 4	124 ± 9	175 ± 13	218 ± 19
Thickness of austenite films (nm)	165 ± 3	212 ± 8	233 ± 11	265 ± 21
Hardness (HV30)	570 ± 10	507 ± 10	480 ± 10	465 ± 10
Impact toughness (J)	8 ± 3	11 ± 3	15 ± 3	19 ± 2

was mainly in a blocky morphology, which could not be effective in the enhancement of impact toughness due to its low mechanical stability and its rapid transformation into martensite during applying the strain. This resulted in the lowest impact toughness value and the brittle nature of the fracture with large fracture facets, as shown in Fig. 7. However, decreasing the cooling rate during the continuous cooling stage of the heat treatment process improved the impact toughness level and the fracture surfaces of the impact specimens showed a much more ductile fracture mode, which was more evident at the lowest cooling rate of 0.1 °C/min, although the differences were not that much considerable. The reduced amount of martensite formed in the microstructure, the increase in the volume fraction of austenite and the replacement of martensite by bainitic sheaves were the main reasons for the improvement in toughness value by reducing the continuous cooling rate from

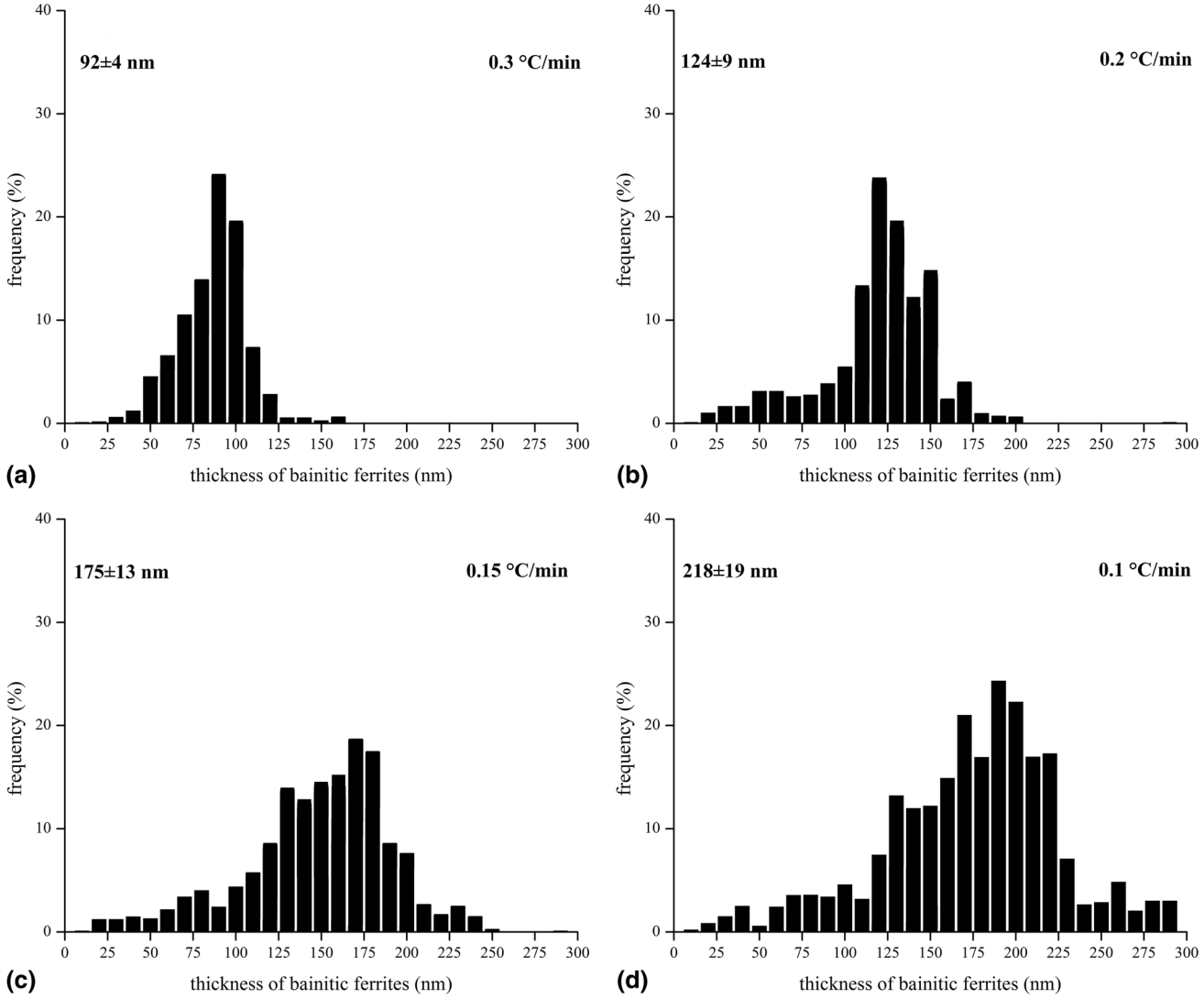

Fig. 6 Size distribution of bainitic ferrites within the microstructures of the heat-treated samples

0.3 to 0.2 °C/min. However, the competing role of the carbon-enriched retained austenite and the volume fraction of bainitic sheaves aligned in different orientations in the microstructure must be considered simultaneously to justify the changes in impact toughness when the cooling rate is further reduced. It was found that reducing the cooling rate from 0.2 to 0.15 and 0.1 °C/min resulted in a lower volume fraction of high carbon retained austenite and lower impact energy values were expected, but the results were in contradiction with the theory. The reason was the positive effect of the higher number of bainitic sheaves formation with different orientations and alignments within the microstructure of the specimens, which was more pronounced at the lowest cooling rate of 0.1 °C/min. Bainitic sheaves had the beneficial effect of restricting the path of crack growth and further improving the impact properties. When sheaves are propagated in different directions within the microstructure, they are more effective in suppressing the crack growth and consequently preventing the early fracture of the specimen. On the other hand, the austenite phase present in the microstructure of the steel at the end of the lower cooling rates was predominantly in a film-like morphology rather than in large blocks. Since the large austenite blocks are thermally and mechanically stable, they cannot play an efficient role in promoting ductility due to an ineffective TRIP effect (Ref 11). It has been shown that the austenite phase must contain nearly 1 wt.% carbon in the solid solution to produce an effective TRIP effect that positively influences ductility (Ref 47). Thus, more mechanically stable austenite and a more effective TRIP effect could also positively influence the toughness properties when the lowest cooling rate is used. In conclusion, a lower amount of martensite, a higher volume fraction of bainitic sheaves of different orientations in the microstructure, and the more mechanically stable retained austenite need to be considered when discussing the impact toughness value in this study.

4. Conclusions

Continuous cooling to achieve a very fine bainitic microstructure in high carbon steel was carried out at different cooling rates. It was shown that continuous annealing can be performed to obtain ultrafine bainite, similar to the isothermal austempering heat treatment process that is commonly used.

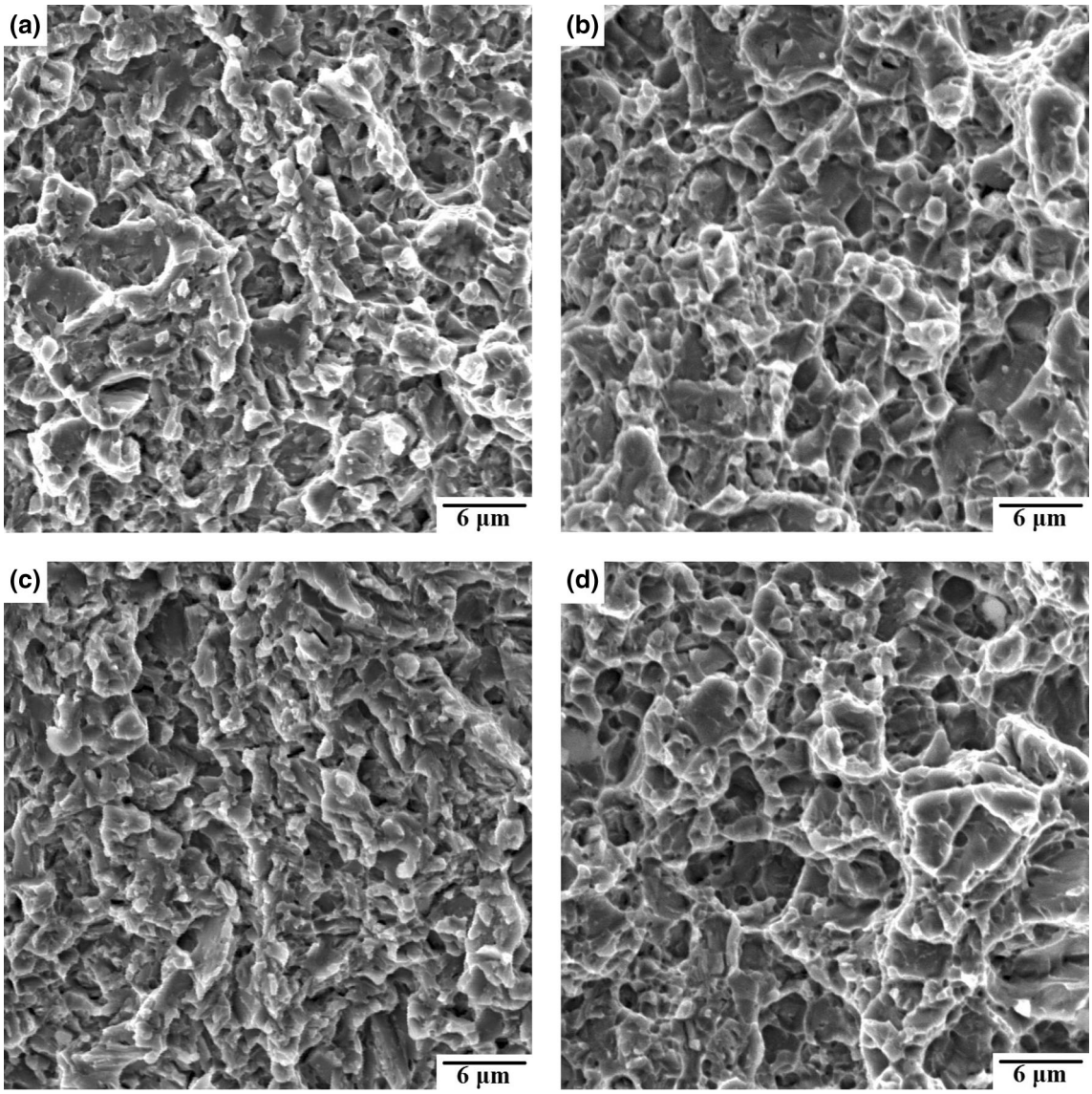

Fig. 7 Fracture surfaces of the Charpy impact test samples which continuously cooled at (a) 0.3 °C/min, (b) 0.2 °C/min, (c) 0.15 °C/min and (d) 0.1 °C/min

The results showed that bainitic ferrites of 92 ± 4, 124 ± 9, 175 ± 13 and 218 ± 19 nm and austenite films of 165 ± 3, 212 ± 8, 233 ± 11 and 265 ± 21 nm thickness could be obtained at the end of cooling rates of 0.3, 0.2, 0.15 and 0.1 °C/min, respectively. The different cooling rates directly affected the size distribution of the bainitic subunits. It was found that decreasing the cooling rate resulted in wider size distribution and larger mean thickness value as the bainite transformation was more advanced and bainitic ferrites of different sizes formed at each different transformation temperature. The hardness of the specimens was directly influenced by the cooling rates, at the end of which different volume fractions of martensite, bainite and austenite phases were achieved in the microstructure. The highest value for the impact toughness was achieved at the lowest cooling rate, as the highest volume fractions of bainitic sheaves with different alignments, a negligible proportion of martensite and mechanically more stable retained austenite formed in the microstructure of the sample.

Acknowledgments

Authors are grateful to Sahand University of Technology for providing the research facilities.

References

1. H.K.D.H. Bhadeshia, *Bainite in Steels*, 2nd ed. Institute of Materials, London, 2001
2. H.K.D.H. Bhadeshia and R.W.K. Honeycombe, Steel, Microstructure and Properties, Butterworths- Heinemann (Elsevier), Amsterdam, 2006
3. X.Y. Long, J. Kang, B. Lv and F.C. Zhang, Carbide-Free Bainite in Medium Carbon Steel, *Mater. Des.*, 2014, **64**, p 237–245
4. M.-X.Zhang and P. M.Kelly, Crystallography of Carbide-Free Bainite in a Hard Bainitic Steel, Mater. Sci. Eng. **438–440**, 272–275 (2006)
5. S. Chatterjee and H.K.D.H. Bhadeshia, Transformation Induced Plasticity Assisted Steels: Stress or Strain Affected Martensitic Transformation, *Mater. Sci. Technol.*, 2007, **23**, p 1101–1104
6. M. Soleimani, A. Kalhor and H. Mirzadeh, Transformation-Induced Plasticity (TRIP) in Advanced Steels: A Review, *Mater. Sci. Eng. A*, 2020, **795**, p 140023

7. C. García-Mateo, F.G. Caballero and H.K.D.H. Bhadeshia, Development of Hard Bainite, *ISIJ Int.*, 2003, **43**, p 1238–1243
8. C. Garcia-Mateo, F.G. Caballero and H.K.D.H. Bhadeshia, Low Temperature Bainite, *J. Phys. IV*, 2003, **112**, p 285–288
9. C. García-Mateo and H.K.D.H. Bhadeshia, Nucleation Theory for High-Carbon Bainite, *Mater. Sci. Eng. A*, 2004, **378**, p 289–292
10. F.G. Caballero, H.K.D.H. Bhadeshia, K.J.A. Mawella, D.G. Jones and P. Brown, Very Strong Low Temperature Bainite, *Mater. Sci. Technol.*, 2002, **18**, p 279–284
11. B. Avishan, S. Yazdani, F.G. Caballero, T. Wang and C. Garcia-Mateo, Characterisation of Microstructure and Mechanical Properties in Two Different Nanostructured Bainitic Steels, *Mater. Sci. Technol.*, 2015, **31**, p 1508–1520
12. B. Avishan, C. Garcia-Mateo, L. Morales-Rivas, S. Yazdani and F.G. Caballero, Strengthening and Mechanical Stability Mechanisms in Nanostructured Bainite, *J. Mater. Sci.*, 2013, **68**, p 6121–6132
13. F.G. Caballero, S. Allain, J. Cornide, J. Puerta Velásquez, C. Garcia-Mateo, and M. Miller, Design of Cold Rolled and Continuous Annealed Carbide-Free Bainitic Steels For Automotive Application, Mater. Des. **49**, 667–680 (2013)
14. B. Avishan, M.A.A. Jani and S. Yazdani, Hardenability of Nanocrystalline Bulk Steel, *Trans. Indian Inst. Met.*, 2018, **71**(2), p 493–503
15. Y.X. Zhou, X.T. Song, J.W. Liang, Y.F. Shen and R.D.K. Misra, Innovative Processing of Obtaining Nanostructured Bainite with High Strength–High Ductility Combination in Low-Carbon-Medium-Mn Steel, *Mater. Sci. Eng. A*, 2018, **718**, p 267–276
16. S. Babu, S. Vogel, C. Garcia-Mateo, B. Clausen, L. Morales-Rivas and F.G. Caballero, Microstructure Evolution During Tensile Deformation of a Nanostructured Bainitic Steel, *Scr. Mater.*, 2013, **69**, p 777–780
17. C. Garcia-Mateo, F.G. Caballero and H.K.D.H. Bhadeshia, Mechanical Properties of Low-Temperature Bainite, *Mater. Sci. Forum*, 2005, **500**, p 495–502
18. W.J. Dan, S.H. Li, W.G. Zhang and Z.Q. Lin, The Effect of Strain-Induced Martensitic Transformation on Mechanical Properties of TRIP Steel, *Mater. Des.*, 2008, **29**, p 604–6012
19. Y.F. Shen, L.N. Qiu, X. Sun, L. Zuo, P.K. Liaw and D. Raabe, Effects of Retained Austenite Volume Fraction, Morphology, and Carbon Content on Strength and Ductility of Nanostructured TRIP-Assisted Steels, *Mater. Sci. Eng. A*, 2015, **636**, p 551–564
20. C. Garcia-Mateo, F.G. Caballero, J. Chao, C. Capdevila and C. Garcia de Andres, Mechanical Stability of Retained Austenite During Plastic Deformation of Super High Strength Carbide Free Bainitic Steels, *J. Mater. Sci.*, 2009, **44**, p 4617–4624
21. P. Jacques, F. Delannay and J. Ladrière, On the Influence of Interactions Between Phases on the Mechanical Stability of Retained Austenite in Transformation-Induced Plasticity Multiphase Steels, *Metall. Mater. Trans. A*, 2001, **32**, p 2759–2768
22. B. Avishan, M. Tavakolian and S. Yazdani, Two-Step Austempering of High Performance Steel with Nanoscale Microstructure, *Mater. Sci. Eng. A*, 2017, **693**, p 178–185
23. J. He, A. Zhao, C. Zhi and H. Fan, Acceleration of Nanobainite Transformation by Multi-Step Ausforming Process, *Scr. Mater.*, 2015, **107**, p 71–74
24. C. Chu, Y. Qin, X. Li, Z. Yang, F. Zhang, C. Guo, X. Long and L. You, Effect of Two-Step Austempering Process on Transformation Kinetics of Nanostructured Bainitic Steel, *Materials*, 2019, **12**, p 166–175
25. H. Mousalou, S. Yazdani, B. Avishan, N.P. Ahmadi, A. Chabok and Y. Pei, Microstructural and Mechanical Properties of Low-Carbon Ultra-Fine Bainitic Steel Produced by Multi-Step Austempering Process, *Mater. Mater. Sci. Eng. A*, 2018, **734**, p 329–337
26. X. Wang, K. Wu, F. Hu, L. Yu and X. Wan, Multi-Step Isothermal Bainitic Transformation In Medium-Carbon Steel, *Scr. Mater.*, 2014, **74**, p 56–59
27. H.K.D.H. Bhadeshia, New Bainitic Steels by Design, Modelling and Simulation for Materials Design, 227–232 (1998)
28. G. Gomez, T. Pérez and H.K.D.H. Bhadeshia, Strong Bainitic Steels by Continuous Cooling Transformation, *New Dev. Metall. Appl. High Strength Steels*, 2008, **2008**(1), p 571–582
29. X. Chen, F. Wang, C. Li and J. Zhang, Dynamic Continuous Cooling Transformation, Microstructure And Mechanical Properties of Medium-Carbon Carbide-Free Bainitic Steel, *High Temp. Mater. Processes*, 2020, **39**, p 304–316
30. L. Morales-Rivas, H. Roelofs, S. Hasler, C. Garcia-Mateo and F.G. Caballero, Complex Microstructural Banding of Continuously Cooled Carbide-Free Bainitic Steels, *Mater. Sci. Forum*, 2014, **783**, p 980–985
31. F.G. Caballero, H.K.D.H. Bhadeshia, K. Mawella, D. Jones and P. Brown, Design of Novel High Strength Bainitic Steels: Part 1, *Mater. Sci. Technol.*, 2001, **17**, p 512–516
32. F.G. Caballero, H.K.D.H. Bhadeshia, K. Mawella, D. Jones and P. Brown, Design of Novel High Strength Bainitic Steels: Part 2, *Mater. Sci. Technol.*, 2001, **17**, p 517–522
33. F.G. Caballero, C. Garcia-Mateo, J. Chao, M.J. Santofimia, C. Capdevila and C.G. De Andres, Effects of Morphology and Stability of Retained Austenite on The Ductility of TRIP-Aided Bainitic Steels, *ISIJ Int.*, 2008, **48**, p 1256–1262
34. P. Clayton and N. Jin, Unlubricated Sliding and Rolling/Sliding Wear Behavior of Continuously Cooled, Low/Medium Carbon Bainitic Steels, *Wear*, 1996, **200**, p 74–82
35. H.K.D.H. Bhadeshia, Advances in the Kinetic Theory of Carbide Precipitation, Mater. Sci. Forum, 35–42 (2003)
36. H.K.D.H. Bhadeshia, M. Lord and L.-E. Svensson, Silicon-Rich Bainitic Steel Welds (Materials, Metallurgy & Weldability, *Trans. JWRI*, 2003, **32**, p 91–96
37. S.H. Song, R.G. Faulkner and P.E.J. Flewitt, Quenching and Tempering-Induced Molybdenum Segregation to Grain Boundaries in a 2.25 Cr–1Mo Steel, *Mater. Sci. Eng. A*, 2000, **281**, p 23–27
38. C. Garcia-Mateo, F.G. Caballero and H.K.D.H. Bhadeshia, Acceleration of Low-Temperature Bainite, *ISIJ Int.*, 2003, **43**, p 1821–1825
39. L.C. Chang and H.K.D.H. Bhadeshia, Austenite Films in Bainitic Microstructures, *Mater. Sci. Technol.*, 1995, **11**, p 874–881
40. B.D. Cullity and S.R. Stock, *Elements of X-Ray diffraction*, 3rd ed. Prentice Hall, NewYork, 2001
41. D.J. Dyson and B. Holmes, Effect of Alloying Additions on the Lattice Parameter of Austenite, *J. Iron. Steel. Inst.*, 1970, **208**, p 469–474
42. H. Matsuda and H.K.D.H. Bhadeshia, Kinetics of the bainite transformation, *Proceedings of the Royal Society of London. Series A: Mathematical, Physical and Engineering Sciences*, 460 (2004) 1707–1722
43. R. Ranjan and S.B. Singh, Isothermal Bainite Transformation In Low-Alloy Steels: Mechanism of Transformation, *Acta. Mater.*, 2021, **202**, p 302–316
44. H.K.D.H. Bhadeshia and J. Christian, Bainite in Steels, *Metall. Trans. A*, 1990, **21**, p 767–797
45. F.G. Caballero, M.K. Miller, C. Garcia-Mateo, J. Cornide and M.J. Santofimia, Temperature Dependence of Carbon Supersaturation of Ferrite in Bainitic Steels, *Scr. Mater.*, 2012, **67**, p 846–849
46. F.G. Caballero, M. Miller, C. Garcia-Mateo and J. Cornide, New Experimental Evidence of the Diffusionless Transformation Nature of Bainite, *J. Alloys Compd.*, 2013, **577**, p 626–630
47. A. Kammouni, W. Saikaly, M. Dumont, C. Marteau, X. Bano and A. Charaï, Effect of the Bainitic Transformation Temperature On Retained Austenite Fraction and Stability in Ti Microalloyed TRIP Steels, *Mater. Sci. Eng. A*, 2009, **518**, p 89–96
48. H.K.D.H. Bhadeshia, Materials Algorithms Project, available at https://www.msm.cam.ac.uk/map/steel/programs/mucg83.html
49. S.B. Singh and H.K.D.H. Bhadeshia, Estimation of Bainite Plate-Thickness in Low-Alloy Steels, *Mater. Sci. Eng. A*, 1998, **245**, p 72–79
50. B. Avishan, S. Yazdani and S.H. Nedjad, Toughness Variations in Nanostructured Bainitic Steels, *Mater. Sci. Eng. A*, 2012, **548**, p 106–111